Numerical simulation of P^+-$InAs_{0.36}Sb_{0.20}P_{0.44}$/ n^0-InAs/n^+-InAs SH-LED for mid-infrared applications

SANJEEV, P. CHAKRABARTI[a*]
Department of Electronics and Instrumentation Engineering, Institute of Engineering and Technology, MJP Rohilkhand University, Bareilly -243 006 India
[a]Centre for Research in Microelectronics (CRME), Department of Electronics Engineering, Institute of Technology, Banaras Hindu University, Varanasi -221 005 India

In this paper, we present ATLAS simulation studies on P^+-$InAs_{0.36}Sb_{0.20}P_{0.44}$/ n^0-InAs/n^+-InAs SH-LED for operation in 2.4–3.5 μm spectral range at room temperature. The device has been characterized in terms of energy band diagram, electric field profile, doping profile, current-voltage characteristics and output power using ATLAS software tool from Silvaco®. The outcomes of the numerical simulations are found to be in good agreement with the reported analytical and experimental results.

(Received September 28, 2009; accepted March 12, 2010)

Keywords: ATLAS, LED, Mid-infrared, Numerical simulation, Heterostructure

1. Introduction

The mid-infrared sources (Light emitting diodes and Injection laser diodes) find applications in a number of areas including optical absorption spectroscopy for detection of pollutant/nuisance and toxic gases [1], next generation optical fiber communication [2-4] and free space optical communication [5]. The sources for mid-infrared spectral range require narrow bandgap semiconductor material for their fabrication. The major constraints in realizing the room temperature continuous operation source are the non-radiative recombination such as Shockley-Read-Hall (SRH) and Auger recombination, which are the dominating recombination mechanisms for narrow bandgap semiconductor material systems, especially at high carrier injection. In the recent past, various structures have been fabricated [6-10] and theoretical models developed for analyzing double heterojunction, single heterojunction and homojunction LEDs [11-13]. These LEDs have been proposed to be used for different target wavelengths in the mid-infrared spectral region. To the best of our knowledge, no ATLAS based simulation studies have been reported for SH-LED operating in mid-infrared spectral region. The paper reports a computer simulation of a single heterojunction LED using commercial software package ATLAS™ from Silvaco® International. The simulation results have been compared and contrasted with those estimated analytically and measured experimentally by others [9].

2. The proposed SH-LED structure

The proposed mid-infrared SH-LED is based on P^+-$InAs_{0.36}Sb_{0.20}P_{0.44}$/ n^0-InAs/ n^+-InAs material system and is similar to one proposed by Krier et al. [9] and analytically modeled by Sanjeev et al. [12]. The schematic of the structure is shown in Fig. 1(a). It consists of a heavily doped (P^+) layer of quaternary materials $InAs_{0.36}Sb_{0.20}P_{0.44}$ of larger bandgap over the undoped InAs layer (active layer) of smaller bandgap to form the heterojunction. The whole structure is supposed to be grown on N^+-InAs substrate of the same conductivity as that of active region material. The energy band diagram of the structure obtained by BLAZE interfaced with ATLAS is shown in Fig. 1(b) and is similar to one reported earlier on the basis of analytical study [12]. The doping profile of the structure is depicted in Fig.1 (c). The ATLAS simulated structure of the device is shown in Fig. 2.

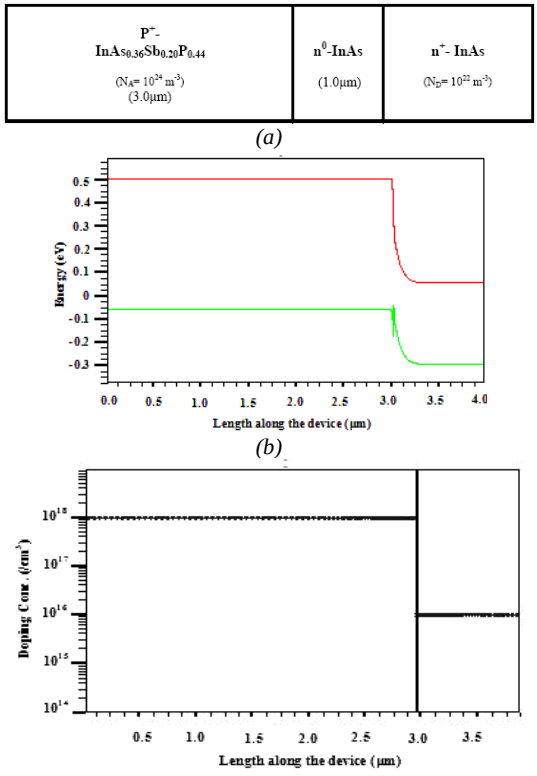

Fig. 1 (a) Schematic of the proposed SH-LED (b) Energy band diagram simulated by ATLAS (c) Doping profile of the structure.

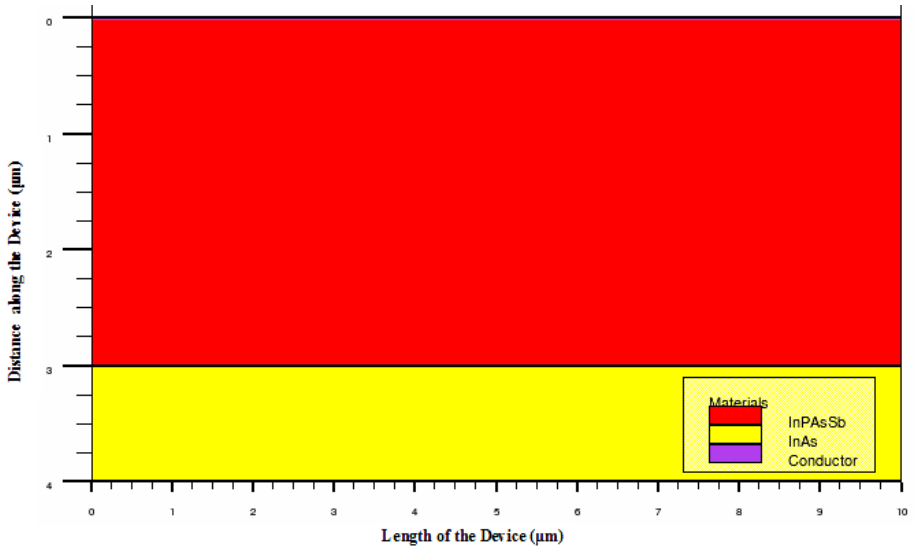

Fig. 2. Schematic of the SH-LED as simulated in ATLAS.

3. ATLAS model for the proposed structure

The analytical model of the trial structure has already been reported [12]. The proposed structure has been simulated in the Deckbuild tool of ATLAS by defining the mesh, region, electrode and doping parameters as given in Table 1. In the material statement, several materials parameters like bandgap, permittivity, density of state of conduction and valance band, mobility and carrier lifetimes value have been provided as per our structure and estimation. We have considered the three most important bulk recombination mechanisms i.e. SRH, AUGER and Band-to-band by considering respective recombination models available in ATLAS [14]. The effect of surface recombination velocity has also been taken into account. The SRH recombination in ATLAS has been modeled as

$$R_{SRH} = \frac{pn - n_{ie}^2}{TAUP0\left[n + n_{ie}\,exp\left(\frac{ETRAP}{kT_L}\right)\right] + TAUN0\left[p + n_{ie}\,exp\left(\frac{-ETRAP}{kT_L}\right)\right]} \quad (1)$$

where $ETRAP$ is the difference between the trap energy level and intrinsic Fermi level, T_L is the lattice temperature in Kelvin and TAUN0 and TAUP0 are the electron and hole lifetimes and are the function of carrier capture cross section and thermal velocity. n , p and n_{ie} are the electron, holes and intrinsic carrier concentration, respectively.

The Auger recombination has been modeled as [14]

$$R_{Auger} = AUGN\left(pn^2 - nn_{ie}^2\right) + AUGP(np^2 + pn_{ie}^2) \quad (2)$$

where $AUGN$ and $AUGP$ are the model parameters defined in the MATERIAL statement in the ATLAS. Apart from the generation and recombination in the bulk of the semiconductor, electrons and holes may be recombining at the heterojunction interface. The so called, surface recombination has been modeled in the ATLAS as

$$R_{Surface} = \frac{pn - n_{ie}^2}{\tau_p^{eff}\left[n + n_{ie}\,exp\left(\frac{ETRAP}{kT_L}\right)\right] + \tau_n^{eff}\left[p + n_{ie}\,exp\left(\frac{-ETRAP}{kT_L}\right)\right]} \quad (3)$$

where

$$\frac{1}{\tau_n^{eff}} = \frac{1}{\tau_n^i} + \frac{d_i}{A_i}S_n \text{ and } \frac{1}{\tau_p^{eff}} = \frac{1}{\tau_p^i} + \frac{d_i}{A_i}S_p \quad (4)$$

here τ_n^{eff} , τ_p^{eff} are the effective value of lifetimes of electrons and holes, τ_n^i and τ_p^i are the electrons and holes bulk recombination lifetimes calculated at i node along the interface, d_i and A_i are the length and area of the interface, S_p and S_n are the surface recombination velocities of holes and electrons at the interface.

The carrier continuity equations for holes for the SH-LED structure under forward bias can be given as

$$\frac{\partial p}{\partial t} = \frac{1}{q}\left(\nabla.\vec{J}_p\right) + G_n - R_n \quad (5)$$

where p is the hole concentration, $\vec{J}_p$ is the hole current density, G_p is the generation rate for holes, R_p is the recombination rate for holes and q is the electronic charge. The equation (5) has been solved numerically by Gummel and Newton methods, which have linear convergence, for the given structure, for finding the hole density in the active region.

The current-voltage characteristics of the structure have been evaluated by solving the governing drift-

diffusion equation under forward bias using initial solution statement in the Deckbuild coding. The energy band diagram of the structure has been drawn using the BLAZE associated with ATLAS. The BLAZE draws the position dependent band structure by modifying the basic charge transport equation of the proposed structure. The energy band diagram, electric field profile, doping profile, electron-hole concentration under equilibrium and current-voltage characteristics have been plotted in the TONYPLOT tool of ATLAS. The output power of the SH-LED has been calculated under high carrier injection condition considering the FERMIDIRAC model of carrier statistics as

$$P = \eta h \nu \left(\frac{I}{q} \right) \tag{6}$$

where η is the quantum efficiency of the LED, I is the bias current.

4. Results and discussion

Numerical computations using ATLAS have been carried out for P^+-$InAs_{0..36}Sb_{0.20}P_{0.44}$/ n^0-InAs/ n^+-InAs single heterostructure light emitting diode (SH-LED) at room temperature. The values of different parameters used in the model are listed in Table 1. Some of the parameters of the quaternary materials (InAsSbP) have been computed from the parameters of the constituent binary/ternary materials using the linear interpolation formula. To a first approximation, the composition dependence of the energy bandgap (Eg_1) of $InAs_xS_byP_{1-x-y}$ at room temperature can be expressed as [15]

$$Eg_1 = xE_g(InAs) + yE_g(InSb) + (1-x-y)E_g(InP) - y(1-x-y)C_2 - x(1-x-y)C_1 - xyC_3 \tag{7}$$

where C_1, C_2 and C_3 are the appropriate bowing parameters for InAs, InSb and InP and $E_g(InAs)$, $E_g(InSb)$ and $E_g(InP)$ are the energy bandgap values of InAs, InSb and InP binary semiconductors respectively at room temperature and are given in Table 1.

Table 1 Values of parameters used in the model [9], [15], [16]

Parameter	Value
N_A	10^{18}cm^{-3}
N_D	10^{16}cm^{-3}
ε_r	15.15
ε_∞	12.3
E_{g1}	0.570 eV (estimated)
E_{g2}	0.354 eV
χ_1	4.699 eV (estimated)
χ_2	4.9 eV
C_1	0.101
C_2	0.20
C_3	0.62
$E_g(InAs)$	0.35 eV
$E_g(InSb)$	0.18 eV
$E_g(InP)$	0.62 eV

Fig. 3 gives the electric field profile across the SH-LED structure under unbiased condition. The electric field abruptly attains a value of $2x10^6$ V/cm at P^+-n^0 heterojunction. From the graph the depletion width of the P^+-n^0 junction can be estimated and which comes out to be $2.5x10^{-7}$ meter which agrees with the value of the depletion width calculated analytically.

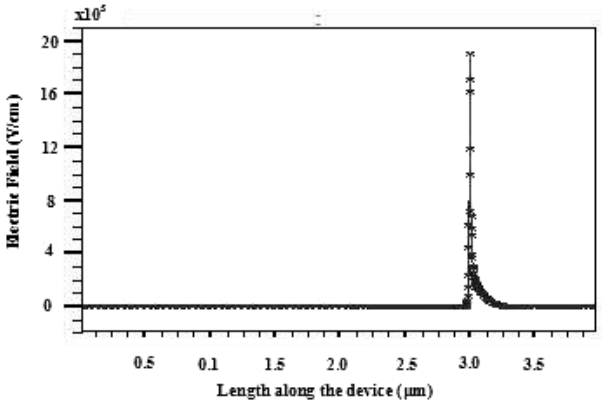

Fig. 3 Electric field profile of the structure.

Fig. 4 gives the electron and hole concentration variation through the structure under unbiased condition. The variation of hole and electron concentration is complimentary to each other throughout the structure, so as to make the diffusion current to be constant within the structure. In the P^+ region, the hole carrier concentration is 10^{18}/cm^2 which decay exponentially to a value of 10^{14}/cm^2 in the n^0 active region. On the other hand the electron concentration of nearly $2x10^9$/cm^2 in the P^+ region goes exponentially to a value of 10^{16}/cm^2 in n^0 active region making it a lightly n-type region. This variation of carrier concentration can be used for estimating the minority carrier lifetimes value which play a very important role in the characterisation of SH-LED at room temperature.

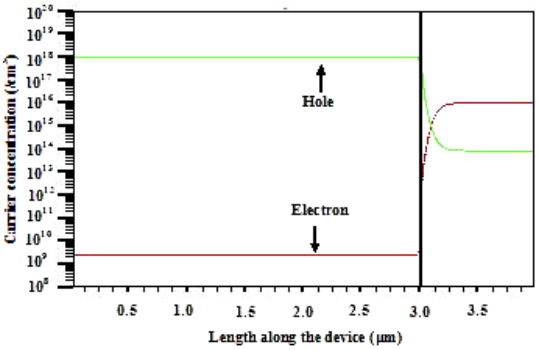

Fig. 4. Electron and hole concentration throughout the structure under no bias condition.

Fig. 5 depicts the forward-bias current-voltage characteristics for the proposed structure evaluated analytically and simulated numerically by ATLAS (shown by circle). There is a good agreement between the simulation results and analytical modeling results for the current-voltage characteristics.

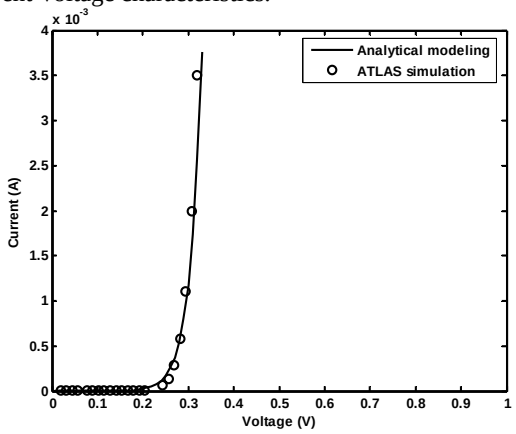

Fig. 5. Forward-bias current-voltage characteristics of the proposed structure.

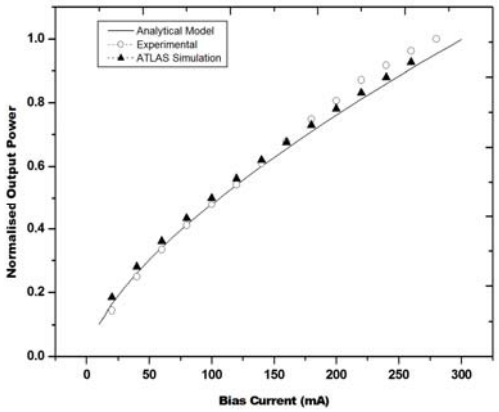

Fig. 6. Bias current and normalized output power of mid-infrared SH-LED.

Fig. 6 illustrate the bias current and normalized output power of mid-infrared SH-LED estimated analytically [12], experimentally [9] and simulated by ATLAS. A good agreement is achieved between analytical model, simulation results and experimental data, which ensures the validity of our proposed ATLAS based model.

5. Conclusions

The numerical simulation have been performed using ATLAS device simulation software for the mid-infrared SH-LED based on P^+-$InAs_{0..36}Sb_{0.20}P_{0.44}$/$n^0$-InAs/$n^+$-InAs material system. Various opto-electrical properties of SH-LED structure have been evaluated and compared with the already reported analytical and experimental results. There is a good agreement between the ATLAS simulation results and reported analytical and experimental results. It is expected that the model developed here, would provide useful design guidelines for the experimentalists for developing new device prototypes.

Acknowledgements

One of the authors (Sanjeev) would like to acknowledge the financial support from the University Grants Commission (UGC), New Delhi in the form of research project for this work.

References

[1] A. Krier, Mid-infrared semiconductor optoelectronics, Springer, 2006.
[2] D. A. Pinnow, A. L. Gentile, A. G. Standlee, A. J. Timper, L.M. Hobrock, Appl. Phys. Lett. **33**, 28 (1978).
[3] L. G. Van Uitert, S. H. Wemple, Appl. Phys. Lett. **33**, 57 (1978).
[4] P. W. France, S. F. Carter, M. W. Moore, C. R Day, British Telecom Tech J. **5**, 28 (1987).
[5] S. Prasad Narasimha, J. Opt. Fiber. Commun. Rep. **2**, 558 (2005).
[6] A. Krier, Phil. Trans. R. Soc. Lond. A **359**, 599 (2001).
[7] A. Krier, V. V. Sherstnev, J. Phy. D: Appl. Phys. **33**, 101 (2000).
[8] H. H. Gao, A. Krier, V. Sherstnev, Y. Yakovlev, J. Phys. D: Appl. Phys. **32**, 1768 (1999).
[9] A. Krier, X. L. Huang, J. Phys. D: Appl. Phys. **39**, 255 (2006).
[10] A. Krier, M. Stone, S. E. Krier, Semicond. Sci. Technol. **22**, 624 (2007).
[11] P. Chakrabarti, V. Saxena, S. K. Das, Y. S. Rao, B. Balaji Lal, Opt. Quant. Electron. **26**, 885 (1994).
[12] Sanjeev, P. Chakrabarti, Optoelectron. Adv. Mater.-Rapid Comm. **2**(8), 459 (2008).
[13] Sanjeev, P. Chakrabarti, Optoelectron. Adv. Mater.-Rapid Comm. **3**(6), 515 (2009).
[14] ATLAS user's manual', Silvaco International, 2005.
[15] E. R Gertner, D. T. Cheung, A. M. Andrews, J. T. Longo, J. Electron. Mater. **6**, 163 (1977).
[16] M. Levinshtein, S. Rumyantsev, M. Shur, Handbook Series on Semiconductor Parameters **1,** World Scientific, 1996.

*Corresponding author: pchakra@bhu.ac.in